A REAL TIME SOLUTION FOR CURRENT TRANSFORMER SATURATION DETECTION BY DISCRETE HAAR WAVELET TRANSFORM

Sukanta DAS

Department of Electrical Engineering, Indian School of Mines, Dhanbad, Jharkhand, India.
E-mail: asksukanta@rediffmail.com, Contact No. +919471191438 (M).

Gautam BANDYOPADHYAY, Prasid SYAM

Department of Electrical Engineering, Bengal Engineering and Science University, Shibpur, Howrah, India.
E-mail: gautamkabi@hotmail.com, prasidsyam@yahoo.co.uk

Chandan JANA

Department of Electrical Engineering, Birbhum Institute of Engineering and Technology, Suri, Birbhum, India.
E-mail: jana_chandan@rediffmail.com

Abstract: *The secondary current of a current transformer (CT) becomes distorted and deviates from the true picture of primary side when a magnetic core enters into saturation. This may lead to severe problem in proper protection decision during transient condition. Wavelet transform with 'Haar' as mother wavelet is used to detect the time instant of core saturation. The multi-resolution analysis of the saturated secondary current of a current transformer is carried out to extract the information of points of inflections. The approach is rigorously verified in MATLAB/SIMULINK environment for initial study and finally the scheme is implemented in real time by DS1104 controller board of dSPACE. Experimental results are shown to validate the detection technique.*

Key words: *CT saturation, detection, Haar, mother wavelet, multi- resolution analysis.*

1. Introduction

A current transformer (CT) is used in power system to scale down the system current signals to an allowable level. If CT characteristic is not properly selected for fault conditions, saturation will occur which may affect the protection decisions [1]-[3]. There are events where it is necessary to locate protection devices far from the CTs. In these cases, the wire resistance, which adds to the CT burden, causes CT saturation at smaller currents than when located close to the protection devices. The distorted secondary current signal of CT may be asymmetrical in nature and may contain DC offset resulting in CT saturation. This leads to incorrect bus-bar differential protection and transformer differential protection in the case of an external fault [2]. For this reason, most low impedance bus-bar differential relays use CT saturation detection unit to avoid false tripping for external faults which may produce large current and significant CT saturation [3]. CT saturation leads to unnecessary delay with IDMT characteristic and coordination may fail. It also creates error in impedance estimation in a distance relay and as a consequence a distance relay can malfunction. Thus, protection relay engineers have to take into account the CT saturation problem when they design a protection relay.

Several approaches may be found in the literature to mitigate or eliminate the impact of CT saturation on protection operation. Detection of CT saturation with the use of algorithmic methods (measurement of certain signal features) has been reported in [4]-[7]. In [4], third difference of saturated CT secondary current has been used as an index of measurement of points of inflection where saturation begins and ends. Paper [5] also uses the third difference of current signal for the aforesaid detection purpose because it is more effective than the second difference in terms of saturation detection. Moreover, this paper includes the effect of a low-pass filter on the proposed algorithm as an anti-aliasing low-pass filter softens the current and, thus, reduces the values of the third difference at those instants. However, a low-pass filter has a tendency to introduce a significant phase shift at the output, thereby causing a delayed detection of points of inflection. A method of symmetrical component analysis for the detection of CT saturation in a numerical current differential feeder protection relay is presented in [6]. However, this paper considers that the probability of CT saturation occurring during a heavy through fault condition only. In [7] wavelet transform, and an artificial intelligence based algorithm for CT saturation detection and compensation has been presented.

This paper proposes a CT saturation detection algorithm based on multi-resolution analysis (MRA) of Haar Transform which is the simplest of transforms. Here, the detail version of two-level decomposition of the detail version of the signal obtained from one-level decomposition successfully detects the points of inflection where saturation begins and ends. The proposed algorithm has been tested in MATLAB/SIMULINK environment over various case studies and finally, the scheme is validated by real time hardware implementation on DS1104 controller board of dSPACE. A 15kHz sampling frequency is chosen for both the simulation and implementation purposes. The result shows expected performance.

2. Methodology for CT saturation detection

In recent years, wavelet transform (WT) techniques have been effectively used for multi-scale representation analysis of signals to demonstrate the local or detailed feature as well as smoothed feature of a particular area of a large signal. For the purpose of implementation, discrete wavelet transform (DWT) has been considered. Using DWT, a signal can be represented as a sum of wavelets and scale functions with coefficients at different time shifts and scales (frequencies) [8]. According to DWT, a time–varying function (signal) $f(t) \in L^2(R)$, the linear vector space of square integrable functions can be expressed in terms of $\phi(t)$ and $\varphi(t)$ as follows

$$f(t) = \sum_k c_{j_0}(k) 2^{-j_0/2} \phi(2^{-j_0} t - k) + \sum_k \sum_{j=j_0} d_j(k) 2^{-j/2} \varphi(2^{-j} t - k) \quad (1)$$

where $\phi(t)$, $\varphi(t)$, c_0 and d_j represent the scaling function, wavelet function, scaling (coarse) coefficient at scale 0 and wavelet (detailed) coefficient at scale *j*, respectively. The symbol *k* is the translation coefficient, which serves for the localization (detection) of a signal for time. The scales *j* = 1, 2, ….denote the different (high to low) frequency bands. The symbol j_0 could be any integer. The translated and scaled (detailed) version of the wavelet, $\varphi(2^{-j}t-k)$, used in the MRA will construct a time-frequency picture of the decomposed signal. $\varphi(t)$ will generate the detailed version of *f(t)*, whereas $\phi(t)$ will generate the coarse version of *f(t)*. It can be shown that

$$c_{j+1}(k) = \sum_m h(m - 2k) c_j(m) \quad (2)$$

$$d_{j+1}(k) = \sum_m g(m - 2k) c_j(m) \quad (3)$$

where $h(m-2k)$ and $g\ (m-2k)$ are the low- and high-pass filters or impulse responses, respectively. Fig. 1(a) illustrates two-scale MRA for a signal, c_0 *[n]* (discrete samples). The symbol *h, g* and '↓ 2' denote low-, high-pass filters and the 'down sampling', respectively [9]. When DWT is applied on a signal taking Daubechies1 ('db1') or 'Haar' as mother wavelet, the process becomes the simplest of transforms which is called the 'Haar Transform' (HT).

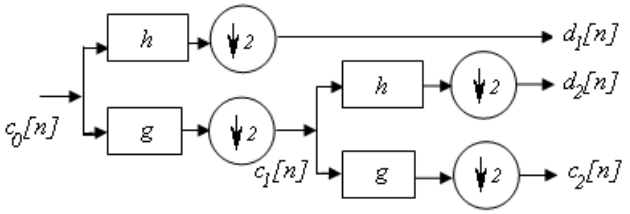

c_0 *[n]* : Original Signal, c_1 *[n],* d_1 *[n]* : Smooth and detail version of the signal c_0 *[n]* at one-level, c_2 *[n],* d_2 *[n]* : Smooth and detail version of the signal c_1 *[n]* at two-level.

(a)

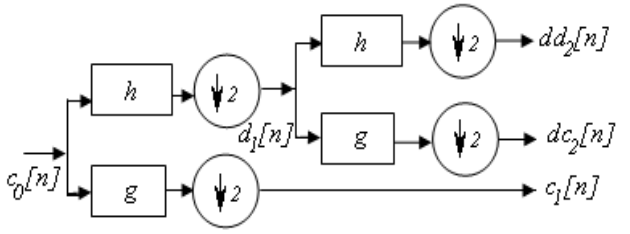

c_0 *[n]* : Original Signal, c_1 *[n],* d_1 *[n]* : Smooth and detail version of the signal c_0 *[n]* at one-level, dc_2 *[n],* dd_2 *[n]* : Smooth and detail version of the signal d_1 *[n]* at two-level.

(b)

Fig. 1. (a) Two-scale MRA for a signal, and (b) Modified two-scale MRA (Wavelet Packet Transform)

The wavelet transform decomposes a signal into different scales with different levels of resolution (both time and frequency) by dilating a single prototype function. It provides a time- local representation (in both time and frequency) of a given signal; therefore, it is suitable for analyzing a signal where frequency resolution is needed such as disturbance transition events in a power quality study [10]. MRA is a powerful tool to decompose a signal *f(t)* into its detailed (indicating sharp changes) and smoothed or scaled versions. A rigorous mathematical treatment of MRA is available in [11].

The HT [11, 12] decomposes a discrete signal into two sub signals of half of its length. One sub-signal is a running average (scaling coefficients) or the smooth signal; the other sub-signal is a running difference (wavelet coefficients) or the detailed signal. Let *f(t)* be a continuous signal and it is sampled by a sample and hold circuits with sampling time T resulting a signal $f^*(t)$ where

$f^*(t) = f(kT) = f_k$, where $t = kT$, k = 0,1, ..*n* (4)

Scaling coefficients or Running average,

$$a_m = \frac{f_{2m-1} + f_{2m}}{\sqrt{2}}, \text{ where m = 1,2, .. } n/2 \qquad (5)$$

Wavelet coefficients or Running difference,

$$b_m = \frac{f_{2m-1} - f_{2m}}{\sqrt{2}}, \text{ where m =1, 2, .. } n/2 \qquad (6)$$

By repeating the process in one level of HT, multiple levels HT can be performed with the application of MRA. In every level, energy of the signal is preserved. Here, only the detail coefficients obtained by MRA are used for saturation detection purpose.

To detect the saturation points (i.e., start and end of saturation in each cycle/points of inflection) HT is applied taking 'Haar' as mother wavelet using modified two-scale MRA (often termed as Wavelet Packet Transform) as shown in Fig. 1(b). In case of detection of points of inflection on saturated CT secondary current, at first, one-level MRA is performed on the signal to get its detailed version ($d_1[n]$) and further one-level decomposition of $d_1[n]$ gives further detailed version of the signal ($dd_2[n]$, Fig. 1(b)). These coefficients ($dd_2[n]$) contain all the information of points of inflections. As 'Haar' is a compactly supported wavelet having only two filter coefficients, therefore, this algorithm can be simply and effectively implemented to detect sudden deviation in the waveform in real time. In Fig. 2(a), scaled primary current and saturated secondary current waveforms are shown. In ideal case, these two waveforms must remain identical in all operating conditions of the CT. But in practice these two waveforms tend to deviate whenever a CT saturates as shown in Fig. 2(a). Here a1, a2, etc are the Start of Saturation (SS) points and b1, b2, etc are the End of Saturation (ES) points in each cycle. Hereinafter, the proposed filter will be termed as Discrete Haar Wavelet Filter (DHWF).

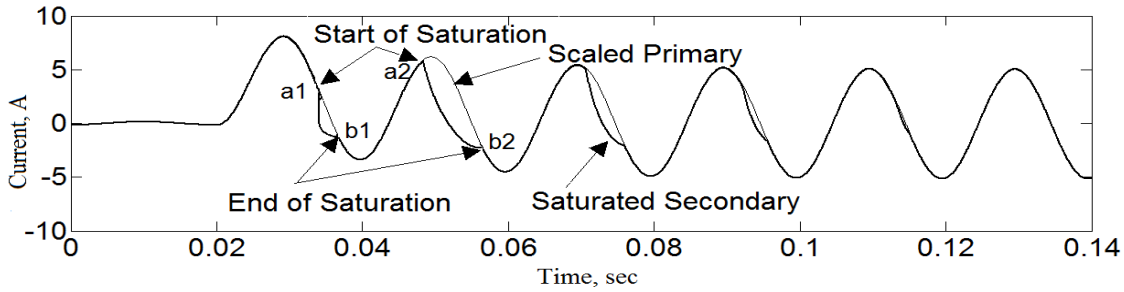

(a)

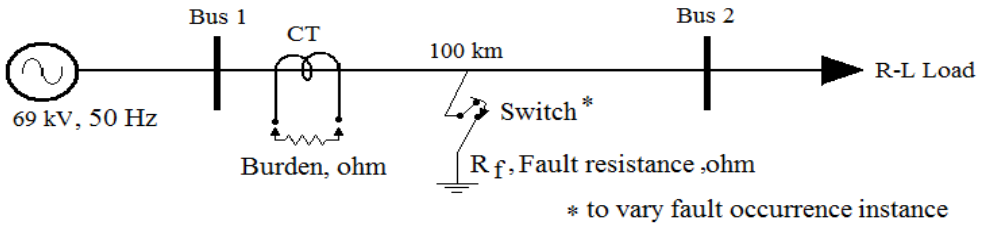

(b)

Fig. 2. (a) Scaled primary current, Saturated secondary current, Start and end of saturation in each cycle, and (b) Sample power system under consideration.

The CT saturation may occur either due to excessive fault current or due to overburden in the CT secondary or due to the presence of DC-offset component in the primary current. The magnitude of DC component depends on the instant at which the fault occurs (i.e., Fault Occurrence Instance, FOI). FOI is measured from the negative to positive zero crossing of voltage waveform. Extensive case studies have been made considering those three different conditions. The proposed scheme is verified by simulation in MATLAB/SIMULINK and the scheme is finally realized using DS1104 controller board of dSPACE. Various case studies have been made and encouraging results are obtained.

3. Scheme for CT saturation detection

Discussed algorithm for CT saturation detection has been developed in MATLAB / SIMULINK and validated under various case studies.

3.1. Simulation of DHWF

Using the saturable CT model (APPENDIX I) in MATLAB/SIMULINK, different saturated CT secondary current waveforms have been generated by varying the CT primary fault current for the sample power system as shown in Fig. 2(b). The fault is created at the instant of zero crossing of the supply voltage from negative to positive. One-level DHWF has been simulated in MATLAB/ SIMULINK [13] environment and the simulation blocks are shown in Fig. 3(a). The saturated CT secondary current signal is fed as input to this filter as analyzing signal.

Pulses 'A' and 'B' as shown in Fig. 3(a) are the sampling pulses for the two Sample and hold (S/H) circuits viz. S/H1 and S/H2 respectively. The filtering process along with the timing diagram is illustrated in Fig. 3(b). Pulse 'A' is formed in the positive going edge of the clock of "Pulse Generator" whose clock frequency is set at 15 kHz. Pulse 'B' is formed in the positive going edge of the clock pulse of the "Divided by 2 counter" and pulse 'C' is formed in the negative going edge of this clock pulse. The outputs of the two S/H circuits (S/H1 and S/H2) are subtracted with a "Subtractor" circuit (Fig. 3(a)). Output of the "Subtractor" circuit is multiplied with a gain of ½ to get detailed version of the analyzing (current) signal using 'Haar' mother wavelet. The output of this "Gain" block is passed through another S/H circuit (S/H3). The sampling signal of this S/H3 is the sampling pulse 'C'. The output of S/H3 is the filtered output at one-level.

Two-level decomposition is comprised of two one-level DHWF modules in cascade as shown in Fig. 3(c). Fig. 3d(ii) shows the sharp changes in magnitude of the Wavelet Transform coefficients (WTCs) at two-level at those points of inflection where saturation of the CT core begins and ends otherwise their values are negligible. The sampling frequency at any level of filtering should be half of that of its preceding level.

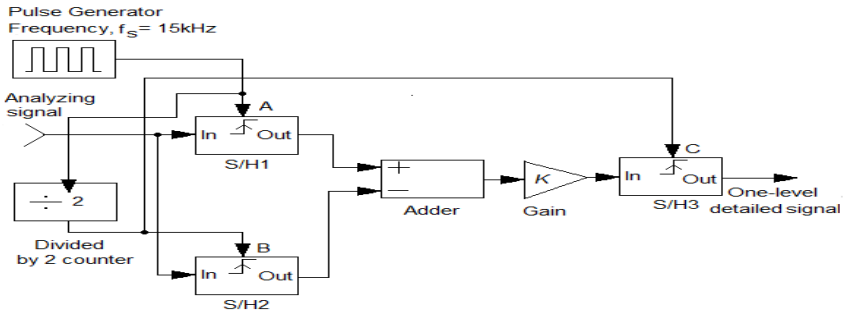

(a)

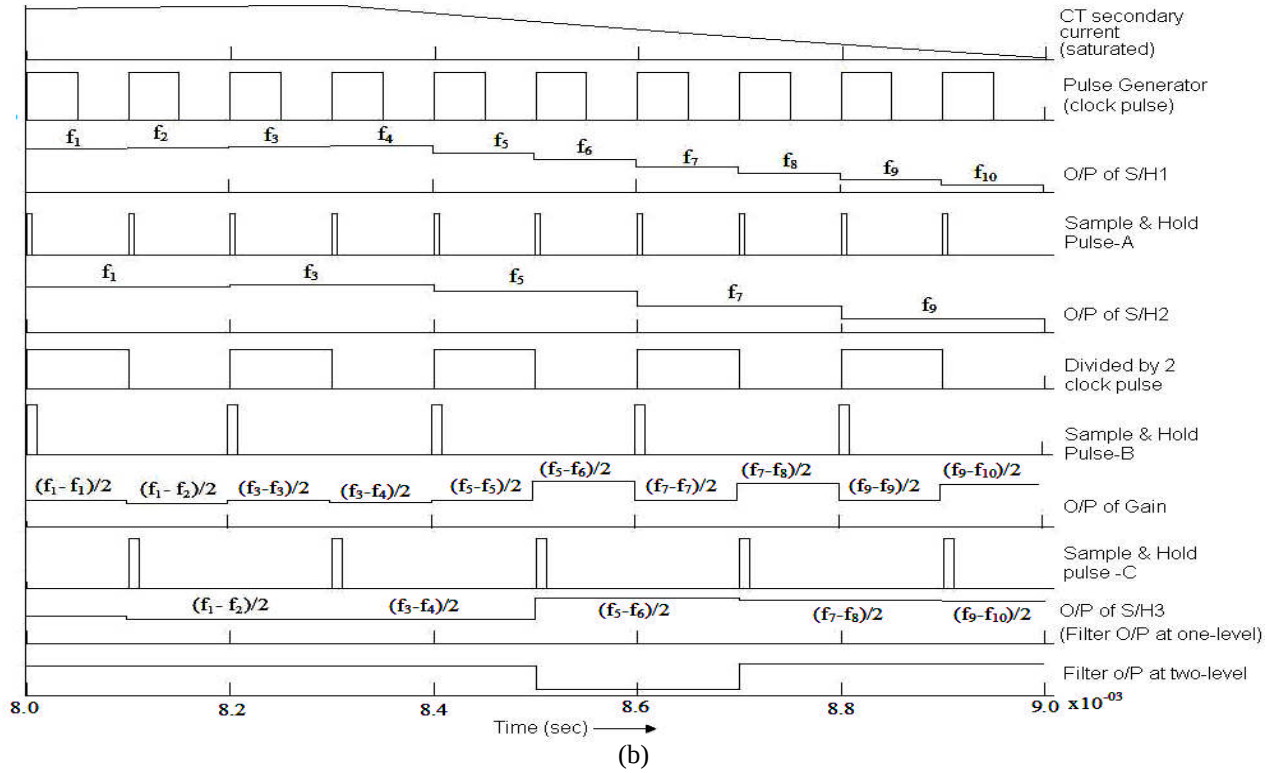

(b)

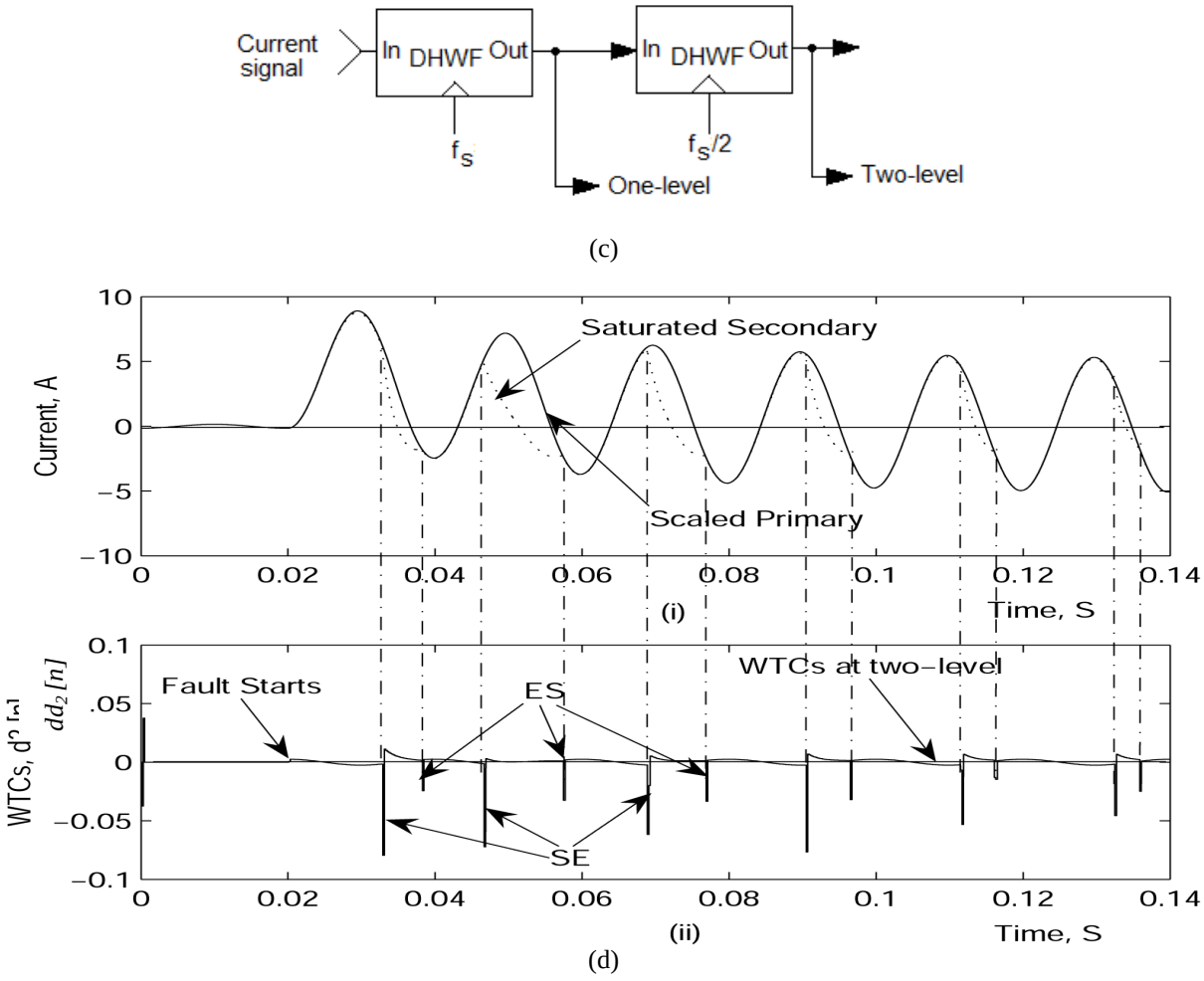

Fig. 3. a) Simulated circuit for one-level DHWF (in detail), (b) Filtering process along with the timing diagram, c)Block diagram to determine two-level detail coefficients, and (d) waveforms for CT saturation detection: i) Scaled Primary current and Saturated Secondary current, and ii)WTCs at Two-level.

3.2. Case studies on CT saturation detection

Extensive case studies have been made for previously mentioned three different conditions keeping other two parameter fixed. Of them three cases have been shown (Fig. 4(ia)-4(iiia)) including the worst CT operating conditions in Fig. 4(iiia). Fig. 4(ib)-4(iiib) show the WTCs, $dd_2\ [n]$ at the points of inflection. Maximum absolute value of WTCs, $|dd_2\ [n]|$ at the points of inflection for first two cycles have been tabulated in Table 1 for these different CT operating conditions.

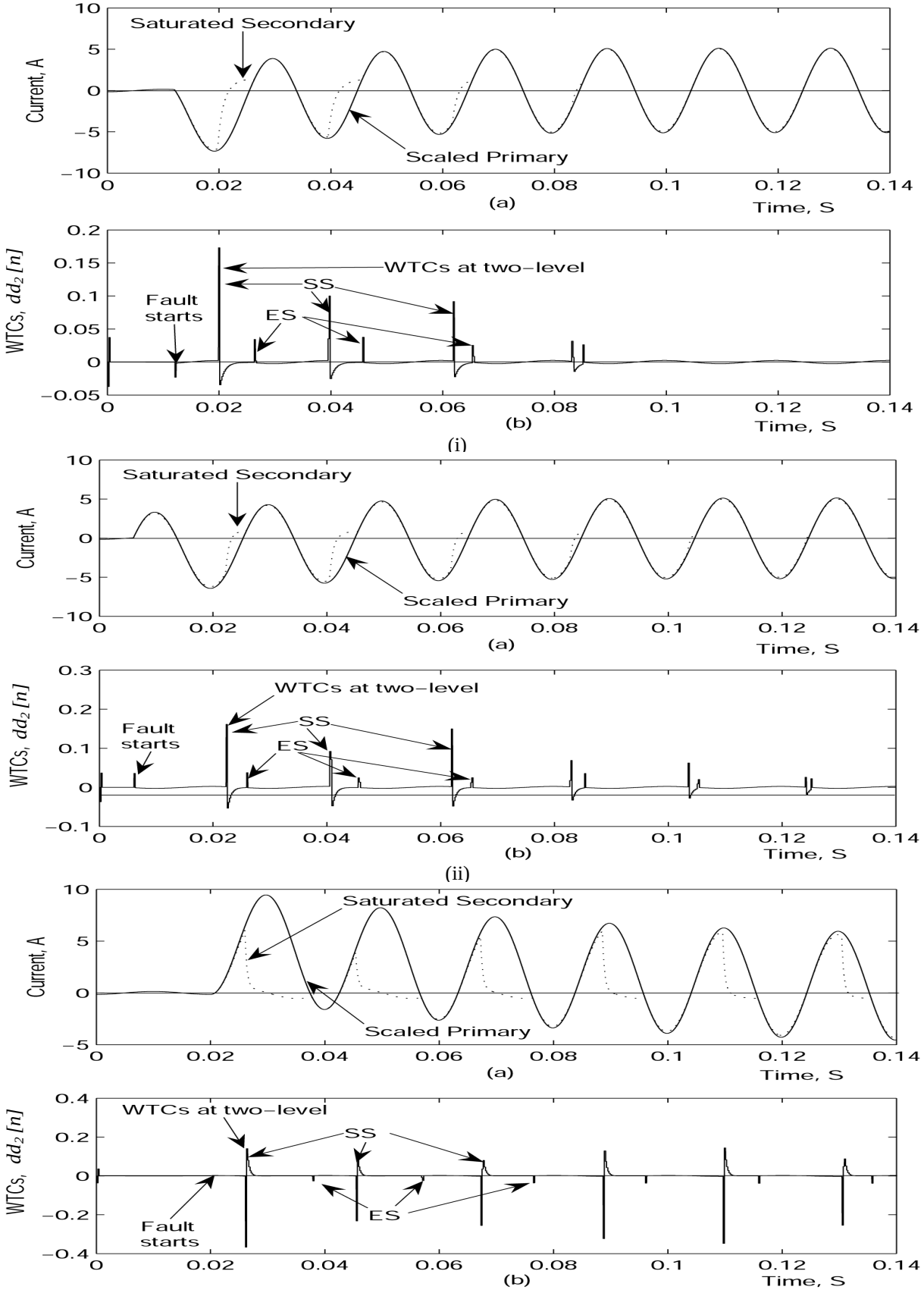

Fig. 4. Case studies on CT saturation detection: i) For R_f =7Ω, FOI = 12ms, Burden =2Ω: a) Scaled primary and saturated secondary current, and b) WTCs, $dd_2[n]$, ii) For R_f =4Ω, FOI = 6ms, Burden =3Ω: Scaled primary and saturated secondary current, and b) WTCs, $dd_2[n]$, and iii) For R_f =1Ω, FOI = 0ms, Burden =5Ω: Scaled primary and saturated secondary current, and b) WTCs, $dd_2[n]$.

Fig. No.	R_f, (Ω)	FOI (ms)	Burden (Ω)	WTCs, $\|dd_2[n]\|$ at points of inflections			
				1st cycle		2nd cycle	
				SS	ES	SS	ES
4(i)	7	12	2	0.2	0.03	0.1	0.04
4(ii)	4	6	3	0.2	0.04	0.1	0.02
4(iii)	1	0	5	0.4	0.03	0.2	0.02

Table 1. Maximum absolute value of WTCs *($|dd_2[n]|$)* at the points of inflection for different CT operating conditions

4. Hardware Implementation

Hardware implementation of the proposed scheme has been done using DS1104 controller board of dSPACE on a saturated CT secondary current.

4.1. DS1104 Controller Board

Fig. 5(a) shows an overview of the architecture and the functional units of the DS1104 [14]. The DS1104 is equipped with two memory sections such as 32-MByte synchronous DRAM (SDRAM) global memory and 8 MByte, divided into 4 blocks of 2 MByte each Flash memory. The DS1104 board is equipped with 6 timer devices driven by the bus clock. The DS1104's main processing unit, MPC8240, consists of a PowerPC 603e microprocessor (master PPC), running at 250 MHz (CPU clock) on which control models are implemented. The master PPC on the DS1104 has 4 parallel ADC (analog-to-digital converter) and 8 parallel DAC (digital-to-analog converter) units with 16-bit resolution and ±10 V input voltage range. The DS1104's slave DSP (Digital Signal Processor) subsystem consists of a Texas Instruments TMS320F240 DSP running at 20 MHz. This DSP provides a timing I/O unit that can be used to generate and measure pulse-width modulated (PWM) and square-wave signals.

4.2. Experimental study

The code for the proposed algorithm for the processor is downloaded through MATLAB/ SIMULINK to which dSPACE controller board is interfaced. The waveforms are captured in plotter of Control Desk Version3.3. CT saturation is achieved with the help of an experimental setup shown in Fig. 5(b). Saturated CT secondary current waveforms were obtained in a 5VA CT by varying burden between 0-26Ω, fault resistance (R_f) between 1-10Ω, load resistance (R) between 0-26Ω and load inductance (L) between 50/100/200mH. The replica of the saturated secondary current waveform is captured as a voltage drop across 1Ω resistance (R_o). Typical waveforms of saturated secondary, corresponding scaled primary current and DHWF output are shown in Fig. 5(c). Experimental results show that the points of inflection on saturated secondary current have been successfully detected. The time taken for detection process is 0.3 ms approximately for 15kHz sampling frequency.

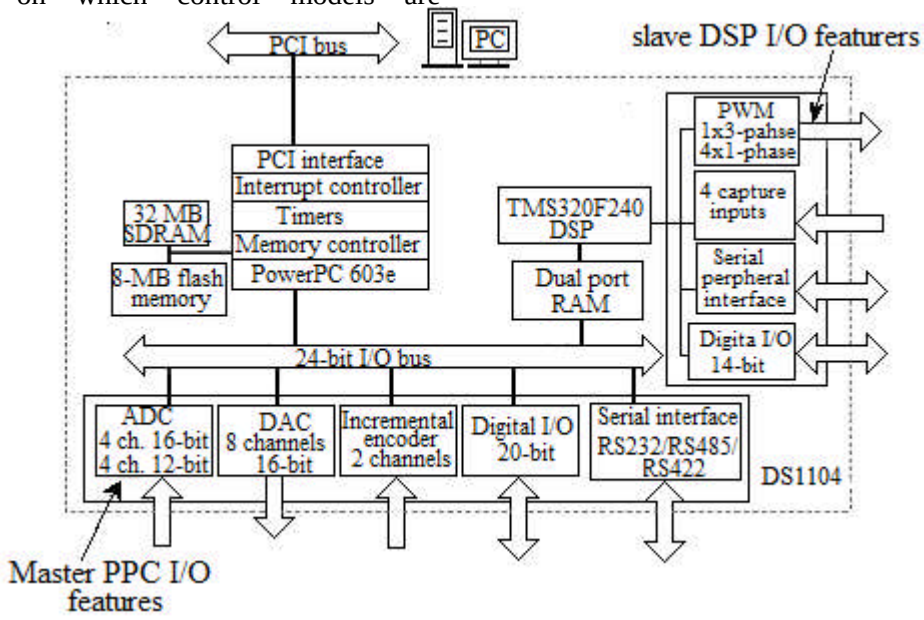

(a)

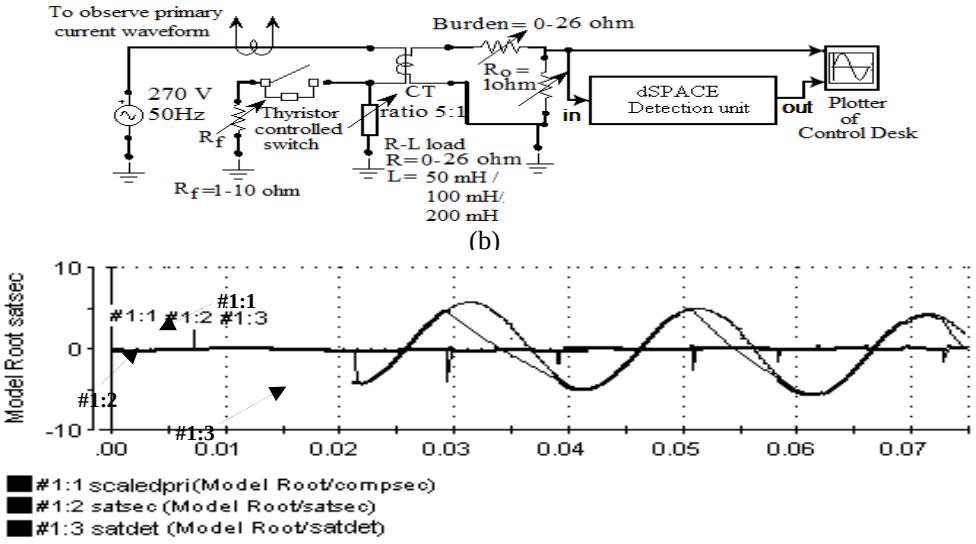

Fig. 5. Real time implementation: a) Block diagram of architecture and functional units of DS1104 controller board, b) A simple experimental set-up to generate saturated secondary current, and c) Scaled primary (scaledpri), Saturated secondary (satsec) and Saturation detected signal (satdet) for FOI ~ 0 ms.

5. Conclusion

This paper demonstrates the application of Haar transform using detail component to detect the points of inflection on the saturated CT secondary current where saturation begins and ends. Unlike [7], Haar is used as mother wavelet which consists of four times less filter coefficients than that of Daubechies 4 mother wavelet, resulting in a very easy real time implementation. The scheme is very simple and it is independent of cut-off frequency of the filter as described in [5]. The proposed method is implemented in real time with DS1104 controller board of dSPACE. The time taken for this detection process is (4/15kHz) 0.3ms which is significantly less without disturbing the protection decisions. Experimental results justify the use of the proposed method of filtering to obtain a satisfactory performance.

APPENDIX

Saturable transformer block model specifications for simulation study:
Type: C400 (2000:5), 25VA, 50Hz; Winding 1, 2
parameters: R_1 (p.u.) =0.001, L_1 (p.u.) =0.04;
Saturation Characteristics (i (p.u.), flux (p.u.)):
[0.0, 0.0; 0.01, 3.0; 1.0, 3.5];
Core loss resistance, Rm (p.u.) =100 ohm.

References

[1] Kjovic Lj.A.: *Impact of current transformer saturation on overcurrent protection operation*. IEEE Power Engineering Society Summer Meeting 2002, July 2002, Vol. 3, p. 1078-1083.

[2] Dave K..: *Evaluation of differential protection relay performance during transformer inrush current & CT saturation period.* 4th Int. conference on Power System Protection and Automation, New Delhi, India, 21-22 Nov. 2007.

[3] Zhang Z., et al: *A novel CT saturation detection algorithm for bus differential protection.* 4th Int. conference on Power System Protection and Automation, New Delhi, India, 21-22 Nov. 2007.

[4] Kang Y., Kang S., Crossley P.: *An algorithm for detecting CT saturation using the secondary current third-derivative function*. Proceedings of the IEEE Bologna Power Tech Conference, 23–26 June 2003, p. 320-326.

[5] Kang Y. C., Ok S. H., Kang S. S. H.: *A CT Saturation Detection Algorithm*. IEEE Transactions On Power Delivery, Vol. 19, No. 1, Jan. 2004, p. 78-85.

[6] Villamagna N., Crossley P. A.: *A CT saturation detection algorithm using symmetrical components for current differential protection*. IEEE Transaction on Power Delivery, Vol. 21 no.1, Jan. 2006, p. 38-45.

[7] Hong Y. Y., Chian P. C.: *Detection and correction of distorted current transformer current using wavelet transform and artificial intelligence.* IET Gener. Transm. Distrib., Vol. 2, No. 4, 2008, p. 566–575.

[8] Burrus, C.S., Gopinath, R.A., Guo, H.; *Introduction to Wavelets and Wavelet Transforms.* Prentice Hall Inc, New Jersey, 1998.

[9] Walker, J. S.: *A primer on Wavelets and their Scientific Applications.* Chapman & Hall/CRC, USA, Hardcover, 1999.

[10] Santoso S., Powers E.J., Grady W.M., Hofmann P.: *Power quality assessment via Wavelet transform analysis.* IEEE Trans on Power Delivery, Vol. 11, No. 2, April 1996, p. 924-930.

[11] Mallat S.: *A theory for multiresolution signal decomposition : the wavelet representation*. IEEE Trans. on Pattern Anal. And Mach. Intell., Vol. 11, July 1989, p. 674-693.

[12] Das S., Syam P., Bandyopahyay G., and Chattopadhyay A. K..: *Wavelet transform application for zero-crossing detection of distorted line voltages in weak AC-systems*. Proc. of IEEE India Annual Conference, INDICON2004, p. 464-467.

[13] MATLAB Release 14 with Service Pack 3 user's guide, The Math Works, Inc. 1994-2005.

[14] DS1104 R&D Controller Board Features, Release 6.3, November 2008, dSPACE GmbH.